inter.noise 2000
The 29th International Congress and Exhibition on Noise Control Engineering
27-30 August 2000, Nice, FRANCE

I-INCE Classification: 2.0

NUMERICAL PREDICTION OF AEROACOUSTIC NOISE RADIATED FROM BALUSTERS OF BUILDINGS WITH LARGE EDDY SIMULATION

T. Oshima*, M. Imano*, T. Sakuma, K. Hirate***

* Department of Architecture, Graduate School of Engineering, the University of Tokyo, 7-3-1, Hongo, Bunkyo-ku, 113-8656, Tokyo, Japan

** Institute of Environment Studies, School of Frontier Science, the University of Tokyo, 7-3-1, Hongo, Bunkyo-ku, 113-8656, Tokyo, Japan

Tel.: +81-3-5841-6176 / Fax: +81-3-5841-8517 / Email: ohshima@env.arch.t.u-tokyo.ac.jp

Keywords:
AEROACOUSTIC NOISE, NUMERICAL PREDICTION, BALUSTERS OF BUILDINGS, LES

ABSTRACT
Sound generation by airflow over square-section balusters of buildings is numerically calculated by a hybrid technique of near-field incompressible flow analysis and far-field integral of Curle equation. Under the conditions of inflow wind velocity of 12 m/s and the side length of the square-section balusters of 21 mm ($\mathrm{Re} = 1.6 \times 10^4$), the result approximately matched an experimental result in peak frequency, which is higher in Strouhal number than the case of an isolated square cylinder in the same Reynolds number.

1 - INTRODUCTION

Reduction of aeroacoustic noise radiated from subsidiaries of buildings like balustrades or louvers are becoming an imperative call due to the growth of living area to windy regions such as high-rise buildings [1]. A quantitative and analytical approach, rather than conventional case-specific experimental studies, to predict the noise and to determine the sound source has been expected as an effective tool for dealing with the problem.
We are working on numerical prediction and analysis of the noise based on Lighthill-Curle acoustic analogy formulation [2], which use a hybrid method of flow analysis and acoustic calculation. In the present study, we present characteristics of the sound radiated by airflow over balusters of buildings.

2 - CALCULATION METHODS

2.1 - Outline

Pure aeroacoustic noise is treated here (no treatment on vibro-acoustic sound is done).
The computational approach utilized in the present study consists of two parts, based on the study of Hardin [3]. First, the incompressible Navier-Stokes equations are solved numerically to give an approximate description of the time-dependent near-field flow dynamics and the acoustic source functions, and then the radiated far-field noise is computed by an appropriate integral over the sound source based on Curle's extension to the Lighthill analogy theory.
The following is the simplified Curle equation assuming low Mach number freestream and far-field approximation,

$$p\left(\mathbf{x},t\right) = -\frac{1}{4\pi c_0}\frac{x_i}{r^2}\frac{\partial}{\partial t}\int f_i\left(\mathbf{y},t-r/c_0\right)dS \tag{1}$$

where c_0 is the velocity of sound in fluid at rest, $\mathbf{x}$ is the receiving point, $\mathbf{y}$ is a point in the source region S, $r = |\mathbf{x}-\mathbf{y}|$, and f_i are the i-direction components of the external forces determined by the flowfield analysis. The discretion of Eq. (1) is calculated numerically giving retarded-time external force variations determined by the flowfield analysis as the source term. In the present study, pressure on the

sound source object is used as the external force (no friction stress component is considered), namely $f_i = n_i p$ where n_i are the direction cosines of the outward normal from the fluid.

2.2 - Flowfield analysis

At low Mach number, it is known that knowledge of the incompressible flow field is sufficient for noise calculations [3]. Thus, for high-Re analysis, the filtered incompressible Navier-Stokes equations with eddy viscosity subgrid-scale stress model (LES) introduced

$$\frac{\partial \bar{u}_i}{x_i} = 0,\ \frac{\partial \bar{u}_i}{\partial t} + \frac{\partial \bar{u}_i \bar{u}_j}{\partial x_j} = -\frac{\partial}{\partial x_i}\left(\bar{p} + \frac{2}{3}k_{SGS}\right) + \frac{\partial}{\partial x_j}\left\{\left(\frac{1}{\mathrm{Re}} + \nu_{SGS}\right)\left(\frac{\partial \bar{u}_i}{\partial x_j} + \frac{\partial \bar{u}_j}{\partial x_i}\right)\right\}$$

(where $\bar{\alpha}$ denotes filtering α at grid scale) are solved numerically. The standard Smagorinsky model is applied for calculating the subgrid-scale stresses.

$$k_{SGS} = \frac{\nu_{SGS}^2}{(C_k\Delta)^2},\ \nu_{SGS} = (C_s\Delta)^2\left(2\bar{S}_{ij}\bar{S}_{ij}\right)^{1/2},\ \bar{S}_{ij} = \frac{1}{2}\left(\frac{\partial \bar{u}_i}{\partial x_j} + \frac{\partial \bar{u}_j}{\partial x_i}\right),\ \Delta = (\Delta_1\Delta_2\Delta_3)^{1/3} f$$

where Δ_i is the grid spacing in the i th direction and f is the Van Driest damping function $f = 1 - \exp(-y^+/26)$ where y^+ is the wall coordinate. The trace of the subgrid-scale stresses k_{SGS} is incorporated in the pressure term in computation and $\bar{p}$ is obtained by subtracting k_{SGS} from the term after the solution is determined. The model coefficients C_k and C_s are chosen to be 0.094 and 0.13 respectively, following former studies [4].

The time-advancement is performed by an explicit SMAC scheme; the convection and the diffusion terms are advanced using the Adams-Bashforth scheme; an MICCG solver is adopted for pressure residual equation. Boundary conditions applied are as follows.

Wall b. c.: Karman's 3-layer generalized log law;

$$\bar{u}_i/u^* = y^+\left(y^+ < 5\right),\ 5\log y^+ - 3.05\left(5 \le y^+ < 30\right),\ 2.5\log y^+ + 5.5\left(5 \le y^+ < 30\right)$$

where u^* is the friction velocity.

Inflow b. c.: the uniform flow; $\bar{u}_i = U_i$ where U_i is the freestream velocity.

Outflow b. c.: convective b. c. with the uniform flow velocity; $\partial \bar{u}_i/\partial t + U_j\left(\partial \bar{u}_i/\partial x_j\right) = 0$.

The spanwise computational domain b. c.: free-slip b. c.

3 - ANALYSIS

The computed model is a balustrade which has 13 square-cylinder-shaped balusters of sectional side length $L = 21$ mm in 130 mm spacing (Fig. 1).

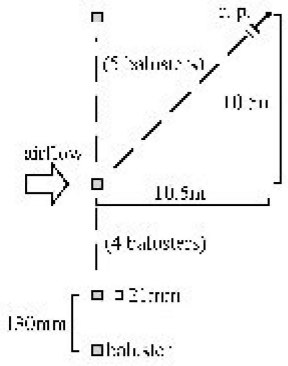

Figure 1: Geometric configuration of sound calculation.

Balusters are modeled as an infinite row of square cylinders by choosing x_2 -directional computational domain length equal to the spacing between balusters and by applying x_2 -directional periodic boundaries in flowfield analysis (Fig. 2). The Reynolds number is chosen to be 1.6×10^4, which corresponds to the freestream velocity $U = 12$ m/s. The uniform inflow is given in right angle to the balustrade. Spanwise computational domain length is chosen to be $2L$ due to the limitation of computational resources. The other computational parameters are described in Tab. 1. The computation is run to nondimensional time $T = 200$ ($t = 0.35$ s).

In sound calculation, simultaneous physical state is assumed around each baluster. The sound receiving point is placed at 10.5 m distance in x_1 - and x_2 -directions from the center of the balustrade.

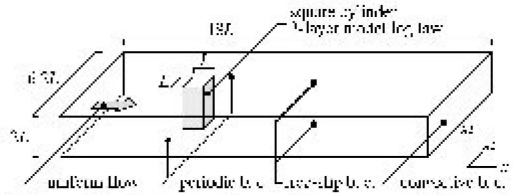

Figure 2: Geometric of computational domain for flow field analysis.

grid	131×101×20 (x_1×x_2×x_3)
minimum grid width	0.017 L
maximum grid width	0.5 L
grid stretching ratio	1.095
ΔT	0.001

Table 1: Computational parameters.

4 - RESULTS

4.1 - Flow region

Fig. 3 shows the isosurface of spanwise velocity component $|u_3| \geq 0.3$ and the pressure contour ($x_3 = L$) at $T = 100$. It is observed that the flowfield contains 3-dimensional turbulence from spanwise velocity component distribution and that the von Kármán vortex street is generated from the square cylinder from the pressure distribution.

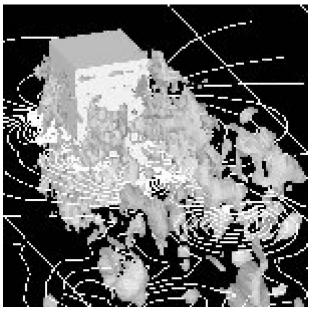

Figure 3: Instantaneous distribution of spanwise velocity component and pressure contour.

4.2 - Sound source

Fig. 4 shows the time histories of drag coefficient C_D and the lift coefficient C_L from $T = 0$ to 100. The root mean square value of the lift coefficient 0.87 is smaller compared to a measured data of the isolated square cylinder shown in ref. [5, 1.2].

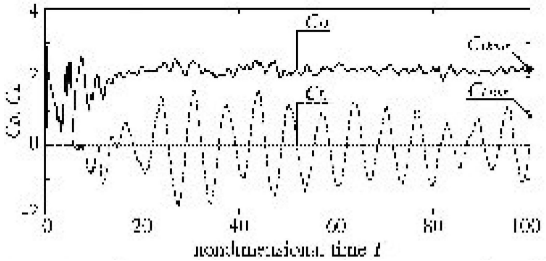

Figure 4: Time histories of drag and lift coefficients.

The spectra of the values of $\partial C_D/\partial t$ and $\partial C_L/\partial t$ as functions of Strouhal number shown in Fig. 5, which correspond to the x_1 - and x_2 -directional sound sources, indicates a strong peak of $\partial C_L/\partial t$ at

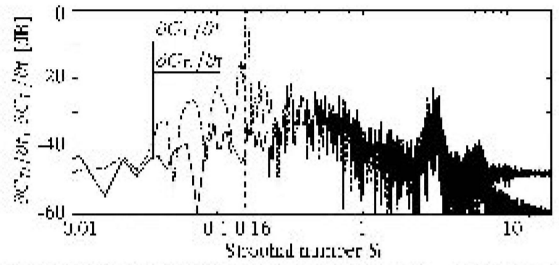

Figure 5: Spectra of time fluctuations of C_D and C_L.

the Strouhal number 0.16 which is higher than the case of an isolated square cylinder, 0.13. Broadband peaks of the both values at 3.0 are also observed.

4.3 - Received sounds

Figs. 6 and 7 show the time histories of the sound at the receiving point calculated with Eq. (1) by giving a single baluster, and all balusters as the sound source respectively. In Fig. 6, a ripple which corresponds to the broadband peak in Fig. 5 is observed over the fundamental wave. A ripple is also observed in Fig. 7, due to a narrowband gain whose frequency corresponds to the difference in retarded-time between the identical sources on the balusters.

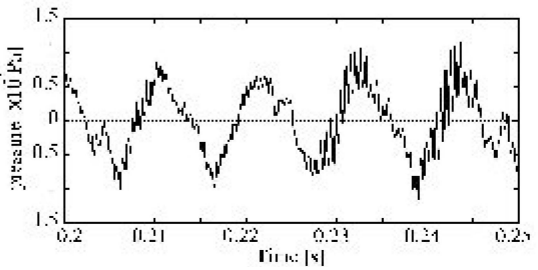

Figure 6: Time history of received sound from a single baluster.

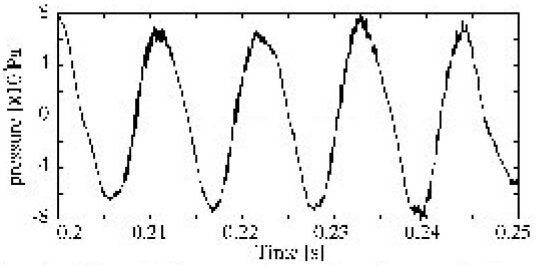

Figure 7: Time history of received sound from all balusters.

The spectra of the sounds as functions of frequency are shown in Fig. 8. The sound from all balusters has a gain in lower frequency compared to the sound from a single baluster. The strongest peak exists at 90 Hz, which approximately matches the experimental result of 100 Hz in 1/3-octave band spectrum shown in ref. [6]. The broadband peak in 3.7 kHz corresponds to the ripple in Fig. 7.

5 - CONCLUSION

Numerical prediction of aeroacoustic noise radiated from airflow of Re=1.6×10^{4} around a balustrade is performed using CFD technique and Lighthill-Curle theory. The peak frequency approximately matched that of an experimental result under the same condition.

Further enhancement of the method, however, is required because the highly simplified modeling of a balustrade in the present study, especially on the assumption of a simultaneous physical state on all balusters, induces artificial gain of the received sound at particular bands.

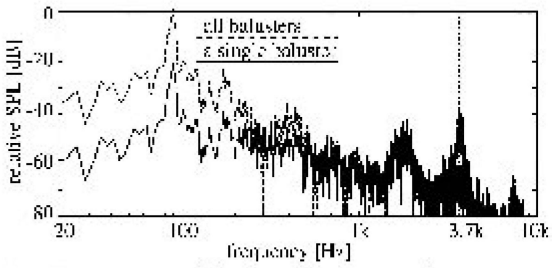

Figure 8: Spectra of the received sounds.

REFERENCES

1. **Kiyoshi YOSHIOKA et al.**, Full-scale measurement and basic study on wind noise in high-rise apartments, *J. of Architecture, Planning and Environmental Engineering (Transactions of AIJ) Tokyo*, Vol. 449, pp. 1-10, 1993

2. **N. Curle**, The influence of solid boundaries upon aerodynamic sound, *Proc. of Roy. Soc., London*, Vol. 231, pp. 505-514, 1955

3. **Jay C. Hardin**, Aeroacoustic computation of Cylinder wake flow, *AIAA J.*, Vol. 22-1, pp. 51-57, 1984

4. **Akashi MOCHIDA et al.**, Comparison between standard and dynamic type of Smagorinsky SGS model, *J. of Architecture, Planning and Environmental Engineering (Transactions of AIJ) Tokyo*, Vol. 479, pp. 41-47, 1996

5. **Shimizu et al.**, Fluid forces working on rectangular-section column-shaped objects, *J. of JSME volume 2, Tokyo*, Vol. 44-384, pp. 2699-2706, 1978

6. **WAKI Takao et al.**, Experimental study of aerodynamic noise of handrail and baluster for building, *Summaries of Technical Papers of Annual Meeting AIJ (Planning), Tokyo*, pp. 83-84, 1984